ELSEVIER

Earth and Planetary Science Letters 181 (2000) 103–114

EPSL

www.elsevier.com/locate/epsl

Experimental evidence for the origin of two kinds of inclusions in diamonds from the deep mantle

Tibor Gasparik [a,*], Mark T. Hutchison [b]

[a] *Center for High Pressure Research and Department of Geosciences, State University of New York at Stony Brook, Stony Brook, NY 11794, USA*

[b] *Lunar and Planetary Laboratory, University of Arizona, Tucson, AZ 85721, USA*

Received 6 January 2000; received in revised form 24 May 2000; accepted 6 June 2000

Abstract

The conditions of origin for the type III inclusions in diamonds from Brazil [Hutchison, Thesis, 1997] and the NaPx–En inclusion from China [Wang and Sueno, Miner. J. 18 (1996) 9–16] were experimentally determined using a split-sphere anvil apparatus (USSA-2000). The type III inclusions formed at a minimum pressure and temperature of 25 GPa and 2000°C, while the origin of the NaPx–En inclusion was close to 23 GPa and 1900°C. Both determinations suggest that the temperature at the corresponding depths is about 300°C higher than predicted by most geotherms for a convecting mantle without a thermal boundary layer at 660 km. Both kinds of inclusions required rapid, single-stage transport by carbonate melt to the Earth's surface, which is consistent with the depths of origin for this melt greater than 660 km. The unusual composition of the NaPx–En inclusion is the result of metasomatism by carbonate melt enriched in Na, K and Mg, and depleted in Si and Al. Since this melt is not kimberlitic in composition, exchange of material between the melt and the mantle was necessary for the melt to become kimberlitic by the time it reached the surface. The resulting metasomatism taking place over a long period of time could cause major changes in the mineral and chemical composition and the structure of the Earth's mantle, and thus play an important role in its evolution.

Keywords: diamond; inclusions; anvil cells; mantle; metasomatism

1. Introduction

There is increasing evidence in support of the deep origin for some inclusions in diamonds, hence such inclusions provide an opportunity to constrain the mineral and chemical composition of the deep mantle directly through their investigation. Here we tentatively define 'deep mantle' as the region between 660 and 1000 km, comprising with the transition zone (410–660 km) Bullen's layer C [3]. Until Moore and Gurney [4] reported the first occurrence of majoritic garnet inclusions in diamonds from South Africa, the evidence from thermobarometry suggested the maximum depth of origin for mantle materials of only about 200 km (e.g. [5]). Since then, inclusions of garnet with significant majorite (pyroxene) content have been reported from a number of localities, but the range of the observed compositions remains sim-

* Corresponding author. Fax: 1-631-632-8140; E-mail: gasparik@sbmp04.ess.sunysb.edu

0012-821X/00/$ – see front matter
PII: S0012-821X(00)00179-5

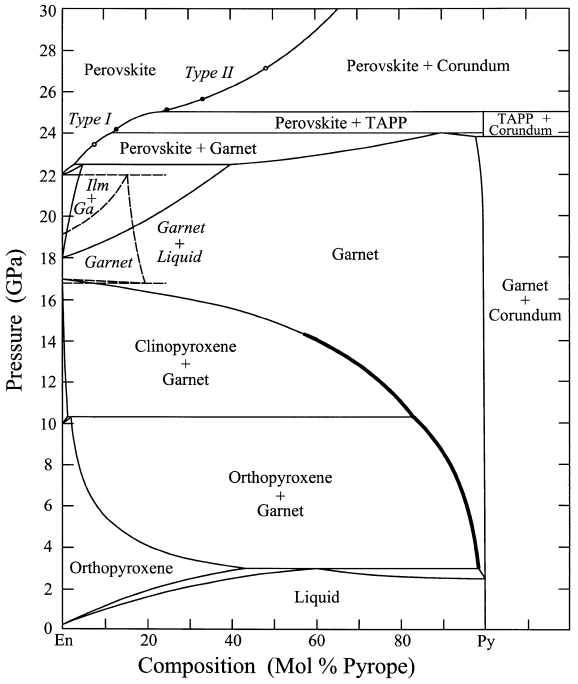

Fig. 1. Pressure–composition phase diagrams for the $Mg_2Si_2O_6$–$Mg_{1.5}AlSi_{1.5}O_6$ (solid line) and $Mg_2Si_2O_6$–$NaMg_{0.5}Si_{2.5}O_6$ (dashed line) joins, approximately at mantle temperatures. The heavy line shows the range of the observed compositions of majoritic garnet inclusions in diamonds from South Africa [4,36], Brazil [1] and Guinea [1]. Also shown are the compositions of the type I and II inclusions in diamonds from Brazil [1], found as single (○) or composite (●) inclusions with TAPP or corundum. The stability field of TAPP is hypothetical. Based on [7,11,37,38].

ilar to that reported in the original paper [4]. It is possible to estimate with confidence from available experimental data [6–8] that the observed range of compositions corresponds to the depths of up to 400 km, assuming coexisting pyroxene (Fig. 1). This assumption is confirmed in some cases by pyroxene inclusions found in association with the majoritic garnet inclusions, for example in diamonds from Brazil and Guinea [1].

Majoritic garnet inclusions with the majorite contents between 43 and 100 mol% have not been found, thus it is possible that none of the majoritic garnet inclusions originated in the transition zone. Hutchison [1] found inclusions with the compositions corresponding to the missing higher majorite contents in diamonds from São Luiz, Brazil, but these inclusions were pyroxenes (described as type I, II and III). Some of them were composite inclusions, where the second phase was either corundum or tetragonal almandine–pyrope phase (TAPP) [9]. Because of this and the association with other non-pyroxene inclusions, such as ferropericlase and wollastonite (which was assumed to form from a $CaSiO_3$ perovskite precursor), Hutchison [1] proposed that these pyroxene inclusions formed originally as $MgSiO_3$ perovskite. If that was the case, some of these inclusions originated at depths exceeding 700 km (Fig. 1).

Among the pyroxene inclusions found by Hutchison [1], four inclusions reported as type III pyroxene had unusual compositions high in Na and low in Ca (Table 1), close to $En_{40}Di_{20}Jd_{40}$ (mol%). Pyroxene with such compositions has not been observed before [1]. However, these compositions are similar to the compositions of majoritic garnet in equilibrium with $CaSiO_3$ perovskite at the transition zone pressures and temperatures, observed by Gasparik [10] during the experimental study of the enstatite–diopside–jadeite system. This suggested that majoritic garnet could be the precursor of the type III inclusions. The composition of such garnet was found to be a sensitive indicator of the equilibration pressures and temperatures [10], and thus suitable for providing constraints on the origin of the type III inclusions.

The NaPx–En inclusion found by Wang and Sueno [2] in a diamond from the Liaoning province, China, has an unusual composition (Table 1) close to 16 mol% $NaMg_{0.5}Si_{2.5}O_6$ (NaPx) and 84% $Mg_2Si_2O_6$ (En). The phase diagram for the NaPx–En join [11] predicted that a phase with this composition should be garnet, requiring for its stability a minimum pressure of 16.5 GPa (Fig. 1). This was recently confirmed by the structure analysis of this inclusion (S. Sueno, personal communication), which showed that the inclusion has the structure of garnet [12]. Since the composition of the inclusion is very close to enstatite, the stability of the NaPx–En garnet must be close to the stability of pure majorite ($Mg_4Si_4O_{12}$). However, its relatively high potassium content (Table 1) suggested that the origin of the NaPx–En inclusion should be near the base of the transition

Table 1
Compositions of the type III [1] and NaPx–En [2] inclusions from diamonds in comparison with the best match from high-pressure experiments (bold)

Cat./6O	237A	242B	246A	259B	**3326**	**3377**	NaPx–En	**3356**	**3412**
Si	2.000	1.915	1.889	1.957	1.994	1.987	2.082	2.091	2.077
Al	0.345	0.517	0.490	0.418	0.449	0.401	0.006	0.001	0.007
Cr	0.087	0.048	0.056	0.036			0.001		
Fe	0.093	0.115	0.131	0.107	0.175	0.176	0.013	0.087	0.011
Mg	0.843	0.849	0.885	0.861	0.763	0.893	1.688	1.627	1.721
Mn	0.014	0.038	0.058	0.033			0.001		
Ca	0.190	0.164	0.174	0.200	0.194	0.181	0.042	0.019	0.020
Na	0.422	0.313	0.307	0.405	0.402	0.345	0.151	0.168	0.160
K	0	0	0	0.001	0.012	0.004	0.012	0.001	0.006
Sum	3.994	3.959	3.990	4.018	3.989	3.987	3.996	3.994	4.002

zone, since significant solubility of potassium in garnet was observed only at pressures above 22 GPa [13]. An explanation for the origin of the NaPx–En inclusion had to account also for its extremely low contents of Al and Fe, which typically are major elements in garnet (Table 1).

Hence, two kinds of inclusions in diamonds with possible origin in the transition zone or the deep mantle were identified. The inclusions have unusual compositions with good potential for providing detailed estimates of equilibration pressures and temperatures in their source regions, and thus were considered to be prime candidates for the determination of their origin by high-pressure experiments.

2. Experimental and analytical techniques

Experiments were carried out with the split-sphere anvil apparatus at the Stony Brook High Pressure Laboratory, using the 10/4 sample assembly with a lanthanum chromite heater [11,14]. The pressure calibration for this assembly has been reported [14–16] and is confirmed in the present study by observations of the $MgSiO_3$ ilmenite to perovskite transition. Accordingly, the sample pressures of 22, 23 and 24 GPa were assigned to gauge pressures of 680, 760 and 900 bar, respectively. The load in metric tons can be obtained by multiplying the gauge pressure by 1.096. To minimize the temperature gradients, shorter 2-mm sample capsules made of rhenium foil were used, as described in [17]. A capsule in this configuration was located slightly off-center, so that the temperature measured by the W3%Re vs. W25%Re thermocouple and reported in Tables 2 and 3 corresponded approximately to the temperature in the cold end of the capsule, while the temperature in the hot spot was about 50°C higher. The temperature was controlled during the experiments by a Eurotherm controller. The experimental procedures were reported in [11].

Starting materials were mechanical mixes of high purity oxides and carbonates obtained commercially, and compounds synthesized for this purpose. The mixes not including Fe were homogenized thoroughly by grinding in an agate mortar under alcohol. Iron was subsequently added as fine metal powder, 325 mesh, and mixed in by hand. After most experiments, some Fe metal was still present, which assured low f_{O_2} in the whole duration of the experiments and minimal Fe^{3+} in the product assemblage [17]. The compositions of the starting materials are listed in Tables 2 and 3.

Experimental products were mounted in epoxy for microprobe analysis. A polished mount contained a lengthwise section of the whole sample still inside the capsule. Wavelength dispersive chemical analyses were obtained with a Cameca electron microprobe using 15 kV accelerating potential, beam current of 10 nA, minimum spot size (1–2 μm), counting time of 10 s, and as standards, natural enstatite for Mg and Si, grossular for Ca

and Al, albite for Na, sanidine for K, and fayalite for Fe. Experimental products were usually well crystallized, with the crystal size exceeding 10 μm. The high quality of the analyses and the minimal Fe^{3+} contents of the analyzed phases are evident from the excellent stoichiometry of the analyses of crystalline phases (Tables 2 and 3). The main criterion for accepting the analyses of crystalline phases with the pyroxene stoichiometry was the sum of cations per 6 oxygens between 3.98 and 4.02. Since all Fe was assumed to be divalent in the calculation of the cations from the wt% of the analyses, higher cation totals would reflect the presence of Fe^{3+}.

Table 2
Experimental conditions and the average phase compositions for experiments on the origin of the type III inclusions

Run	Mix[a]	*t*	*P*	*T*	Phase[b]	An.[c]	Cations/6 oxygens							Sum	CO_2
		(h)	(GPa)	(°C)			K	Na	Ca	Fe	Mg	Al	Si		(wt%)
3281	A	1	23	1600	Ga	22	0	0.243	0.119	0.262	1.132	0.272	1.979	4.007	
					CaPv	5	0	0.025	1.955	0.014	0.003	0.007	2.002	4.006	
					Rw	8	0	0.016	0.004	0.830	2.171	0.003	1.491	4.515	
3291	B	2	23	1600	Ga	13	0	0.302	0.097	0	1.308	0.289	2.005	4.001	
					CaPv	1	0	0.049	1.944	0	0.022	0.023	1.987	4.025	
					Ilm	8	0	0.014	0	0	1.966	0.013	2.004	3.997	
					MgPv	3	0	0.015	0.003	0	1.978	0.017	1.993	4.006	
3305	C	2	23	1600	Ga	27	0	0.390	0.136	0.188	0.880	0.424	1.982	4.000	
					CaPv	5	0	0.034	1.922	0.015	0.022	0.029	1.990	4.012	
3309	D	2	23	1600	Ga	6	0.006	0.338	0.103	0.172	1.083	0.232	2.061	3.995	
					CaPv	4	0.016	0.025	1.938	0.014	0.010	0.011	2.000	4.014	
					MgPv	5	0.003	0.028	0.032	0.262	1.653	0.053	1.979	4.010	
					Rw	3	0.008	0.015	0.007	0.662	2.322	0.002	1.497	4.513	
					K-p	1	0.948	0.153	0.010	0.276	1.558	0.013	1.792	4.750	
3316	D	2	22.5	1700	Ga	14	0.009	0.172	0.131	0.251	1.236	0.209	1.989	3.997	
					CaPv	6	0.009	0.010	1.883	0.017	0.068	0.013	2.002	4.002	
					MgPv	5	0.002	0.023	0.116	0.241	1.618	0.030	1.983	4.013	
3318	C	2	22	1700	Ga	20	0	0.379	0.178	0.155	0.876	0.443	1.969	4.000	
					CaPv	6	0	0.021	1.953	0.014	0.012	0.020	1.990	4.010	
3326	E	2	22	1700	Ga	10	0.012	0.402	0.194	0.175	0.763	0.449	1.994	3.989	
					CaPv	5	0.035	0.001	1.923	0.010	0.007	0.005	2.017	3.998	
					K-p	3	0.721	0.369	0.010	0.307	1.457	0.030	1.818	4.712	
3359	E	2	22	1800	Ga	22	0.004	0.380	0.206	0.148	0.836	0.429	1.987	3.990	
					CaPv	2	0.033	0.035	1.891	0.019	0.030	0.045	1.979	4.032	
3368	E	2	23	1800	Ga	5	0.005	0.391	0.193	0.162	0.808	0.424	2.002	3.985	
					CaPv	5	0.012	0.010	1.958	0.011	0.004	0.006	2.004	4.005	
3372	D	2	24	1900	Ga	13	0.003	0.104	0.164	0.207	1.371	0.236	1.925	4.010	
					CaPv	3	0.005	0.003	1.937	0.013	0.015	0.007	2.011	3.991	
					MgPv	2	0.002	0.014	0.086	0.246	1.687	0.085	1.923	4.043	
					K-h	1	0.636	0.025	0.016	0.028	0.131	0.683	2.235	3.754	
					L	12	1.012	0.678	0.556	0.457	1.254	0.105	1.365	5.427	29
3377	E	2	24	1900	Ga	21	0.004	0.345	0.181	0.176	0.893	0.401	1.987	3.987	
					CaPv	3	0.010	0.029	1.835	0.035	0.063	0.015	2.012	3.999	
					K-h	4	0.649	0.054	0.014	0.020	0.046	0.619	2.320	3.722	
					L	11	0.319	1.007	0.360	0.386	0.668	0.229	1.789	4.758	20

[a]Starting materials (in mol): A = 10 SiO_2, 7 MgO, 7 $CaSiO_3$, 3 $NaAlSiO_4$, 5 $Mg(OH)_2$, 2 $Na_2Si_2O_5$, 3 Fe°; B = Fe-free A; C = A+2 Fe°; D = 10 SiO_2, 9 MgO, 9 $CaSiO_3$, 1 $NaAlSiO_4$, 1 $MgCO_3$, 1 Na_2CO_3, 1 K_2CO_3, 2 Fe°; E = 13.8 SiO_2, 9.5 MgO, 7.9 $CaSiO_3$, 4.3 $NaAlSiO_4$, 2 Na_2CO_3, 1 K_2CO_3, 2 Fe°.

[b]CaPv = $CaSiO_3$ perovskite, Ga = garnet, Ilm = $MgSiO_3$ ilmenite, K-h = K-hollandite, K-p = a new K-rich phase, L = quenched liquid, MgPv = $MgSiO_3$ perovskite, Rw = Mg_2SiO_4 ringwoodite.

[c]The total number of microprobe analyses accepted from the given experiment for each phase.

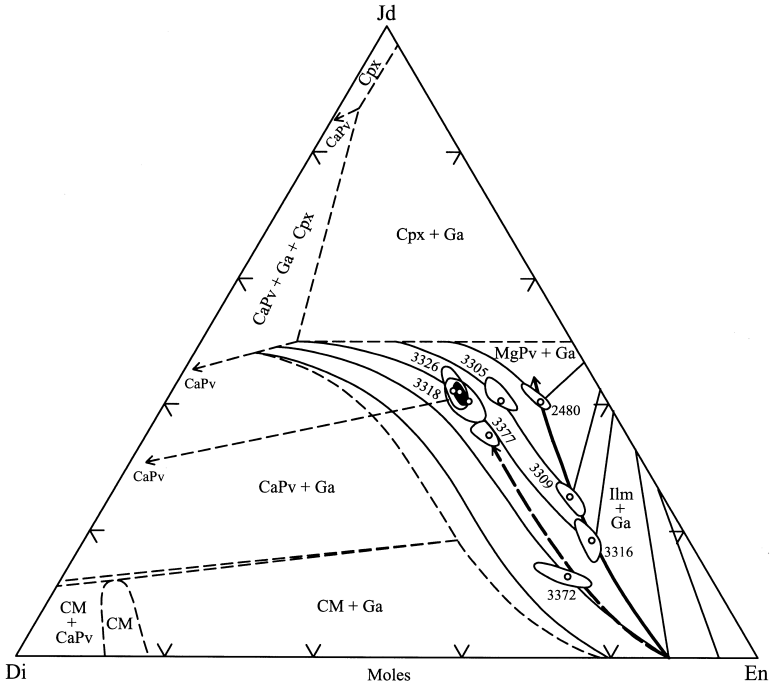

Fig. 2. Schematic phase relations for the system enstatite–diopside–jadeite, based on [10]. Thin lines are isobars (solid), tie-lines and the limits of garnet stability (dashed). Heavy lines are the loci of the compositions of garnet coexisting with $CaSiO_3$ perovskite, and either $MgSiO_3$ ilmenite at low pressure and temperature (solid) or $MgSiO_3$ perovskite at relatively higher pressure and temperature (dashed). The solid envelope encloses the observed average compositions of the Type III inclusions, open envelopes enclose the compositions of garnet from experiments in Table 2, identified by their run numbers, with circles indicating average compositions. Symbols: CaPv, $CaSiO_3$ perovskite; CM, CM phase; Cpx, clinopyroxene; Di, diopside; En, enstatite; Ga, garnet; Ilm, $MgSiO_3$ ilmenite; Jd, jadeite; MgPv, $MgSiO_3$ perovskite.

3. Experimental results on the origin of the type III inclusions

The results from the experiments on the origin of the type III inclusions are summarized in Table 2 and Fig. 2. The phase relations determined in the experimental study of the enstatite–diopside–jadeite system [10] served as a suitable starting point in the task of matching the composition of the type III inclusions. It was expected that the majoritic garnet with the type III composition coexisted not only with $CaSiO_3$ perovskite, but also with $MgSiO_3$ ilmenite or perovskite. Such assemblages should be typical for the transition zone or the top of the deep mantle for a wide range of possible mantle compositions. For example, Fig. 2 shows the composition of garnet in equilibrium with $CaSiO_3$ perovskite and $MgSiO_3$ ilmenite at 22 GPa and 1500°C (run 2480), as was reported in [10]. Such garnet compositions would lie on the heavy solid line in Fig. 2, while the heavy dashed line indicates the compositions of garnet coexisting with two perovskites at relatively higher pressures and temperatures. The composition of garnet in such assemblages is a sensitive indicator of the equilibration pressures and temperatures, because the Ca content is primarily temperature-dependent, while the Na content is mostly a function of pressure [10].

Since the study of Gasparik [10] did not include Fe, additional experiments with Fe-bearing compositions closer in chemistry to the type III inclusions were carried out to verify the effect of Fe on the phase relations. For this we used a starting material from [10], which was known to produce the appropriate assemblage and phase compositions (run 2480), and added to it Fe metal powder. The first two experiments in Table 2 (runs

3281 and 3291) demonstrated that the effect of Fe was minimal. The composition of garnet coexisting with $CaSiO_3$ perovskite only, obtained at 23 GPa and 1600°C (run 3305), was close to the average composition of the type III inclusions, but clearly did not match it. The composition of garnet coexisting with 2 perovskites at the same conditions (run 3309) had substantially lower Na content, making it evident that the inclusions could not coexist with a $MgSiO_3$ phase at those conditions. It also became obvious that in order to match the Ca content of the type III inclusions, it was necessary to raise the temperature. The composition was then matched at 22 GPa and 1700°C (run 3318), but only in the presence of $CaSiO_3$ perovskite. However, the range of the observed garnet compositions was too large, indicating problems with reaching equilibrium. A new

Table 3
Experimental conditions and the average phase compositions for experiments on the origin of the NaPx–En inclusion

Run	Mix[a]	*t*	*P*	*T*	Phase[b]	An.[c]	Cations/6 oxygens							Sum	CO_2
		(h)	(GPa)	(°C)			K	Na	Ca	Fe	Mg	Al	Si		(wt%)
3288	F	2	23	1600	MgPv	16	0.005	0.019	0.009	0.311	1.698	0.074	1.929	4.045	
					Rw	9	0.008	0.028	0.003	0.857	2.093	0.008	1.509	4.506	
					St	1	0.002	0	0	0.010	0.002	0.018	2.980	3.012	
					K-p	4	0.842	0.159	0.005	0.386	1.448	0.026	1.811	4.677	
					K-h	3	0.720	0.018	0.001	0.029	0.099	0.515	2.365	3.747	
					L	10	1.481	1.866	0.548	0.728	1.111	0.119	0.881	6.733	33
3297	F	2	22	1600	Ilm	9	0	0.003	0	0.090	1.907	0.002	1.998	4.000	
					Ga	13	0.003	0.063	0.044	0.222	1.583	0.116	1.972	4.003	
					Rw	8	0.001	0.005	0.001	0.436	2.557	0.001	1.501	4.502	
					St	1	0.001	0	0	0.011	0	0.010	2.986	3.008	
					L	10	0.986	0.147	0.148	0.690	1.564	0.131	1.418	5.084	33
3352	G+H	2	21	1800	Ilm	8	0	0.005	0	0.017	1.944	0	2.018	3.984	
					Ga	7	0	0.109	0.004	0.037	1.796	0.001	2.054	4.001	
					Ga	15	0	0.168	0.006	0.042	1.678	0.001	2.094	3.989	
					St	1	0	0.003	0	0.002	0	0.006	2.994	3.005	
					L	7	0.366	3.859	0.135	0.083	3.369	0.014	0.140	7.966	53
3356	G+H	2	22	1800	Ilm	11	0	0.006	0	0.044	1.940	0	2.006	3.996	
					Ga	11	0.001	0.151	0.017	0.075	1.681	0.001	2.074	4.000	
					Ga	21	0.001	0.168	0.019	0.087	1.627	0.001	2.091	3.994	
					St	1	0	0	0	0	0	0.001	2.999	3.000	
					L	11	0.488	3.661	0.256	0.226	2.559	0.017	0.429	7.636	44
3390	G+H	2	23	2000	MgPv	6	0	0.020	0	0.043	1.915	0	2.016	3.994	
					Ga	6	0	0.094	0.005	0.011	1.813	0.001	2.061	3.985	
					St	1	0	0	0	0	0	0.002	2.998	3.000	
					L	5	0.005	0.249	0.020	0.028	1.992	0.032	1.893	4.219	7
3408	G+I	0.1	24	2000	MgPv	3	0.004	0.013	0.002	0.010	1.974	0.004	2.000	4.007	
					St	2	0.003	0.004	0	0.001	0	0.004	2.995	3.007	
3412	G+I	0.1	23	1900	MgPv	7	0.001	0.016	0.002	0.005	1.966	0.002	2.007	3.999	
					Ga	11	0.006	0.160	0.020	0.011	1.721	0.007	2.077	4.002	
					St	1	0.001	0.002	0	0	0	0.015	2.988	3.006	
3433	G+F	1	23	1900	MgPv	5	0	0.022	0.001	0.048	1.904	0.008	2.012	3.995	
					Ga	21	0	0.206	0.006	0.055	1.614	0.006	2.107	3.994	
					St	3	0	0	0	0.002	0	0.003	2.996	3.001	
					L	13	0.164	1.473	0.049	0.218	1.812	0.080	1.492	5.288	32

[a]Starting materials (in mol): F = 10 SiO_2, 8 MgO, 0.2 $CaSiO_3$, 0.4 $NaAlSiO_4$, 0.3 $Na_2Si_2O_5$, 1 $MgCO_3$, 0.5 K_2CO_3, 2 Fe°; G = 18 SiO_2, 14 MgO, 2 $Na_2Si_2O_5$; H = 52 SiO_2, 64 MgO, 1 $CaSiO_3$, 1.6 $Na_2Si_2O_5$, 3 $MgCO_3$, 1.6 K_2CO_3, 4 Fe°; I = 50 SiO_2, 70 MgO, 5 $CaCO_3$, 5 Na_2CO_3, 10 K_2CO_3, 2 Fe°.

[b]Ga = garnet, Ilm = $MgSiO_3$ ilmenite, K-h = K-hollandite, K-p = K-rich phase, L = quenched liquid, MgPv = $MgSiO_3$ perovskite, Rw = Mg_2SiO_4 ringwoodite, St = stishovite.

[c]The total number of microprobe analyses accepted from the given experiment for each phase.

starting material with a carbonate flux produced almost identical results (run 3326), but the range of the observed garnet compositions was much narrower and thus more satisfactory in demonstrating the achievement of equilibrium. The Ca content of the type III inclusions was also matched at 23 GPa, 1800°C (run 3368) and at 24 GPa, 1900°C (run 3377), but only in the presence of $CaSiO_3$ perovskite and still in the stability field of pyrope. In contrast, one of the type III inclusions was found in contact with TAPP, presumably indicating pressures higher than the stability of pyrope [9]. This suggested that the type III garnet coexisting with 2 perovskites and TAPP could become stable at 25 GPa and 2000°C or higher pressures and temperatures.

4. Experimental results on the origin of the NaPx–En inclusion

The results from the experiments on the origin of the NaPx–En inclusion are summarized in Table 3. A plausible explanation of its origin had to account for the unusual composition (Table 1), particularly the relatively high contents of Na and K, and the extremely low contents of Al and Fe. To obtain some answers, the experimental study was expanded to carbonate-bearing systems to explore the possible role of carbonate melt in the origin of this and other inclusions. Preliminary experiments at 1600°C (Table 3) showed that very low Fe contents were imposed on $(Mg,Fe)SiO_3$ ilmenite or perovskite by coexisting $(Mg,Fe)_2SiO_4$ ringwoodite and stishovite or carbonate melt at 22–23 GPa, thus suggesting a possible reason for the extremely low Fe content of the NaPx–En inclusion. In addition, K, Na, Ca, Fe and Mg strongly partitioned into carbonate melt, while the melt was depleted in Si and Al, suggesting the reason for the low Al content of the inclusion. It also became obvious that much higher Na contents were necessary in the starting material to match the relatively high Na content of the inclusion.

The remaining experiments were carried out using the 'sandwich technique', in which most of the sample consisted of a starting material with the composition $NaPx_{40}En_{60}$ (mol%), and a small amount of a carbonate-bearing mix was placed in the hot spot of the sample capsule (Table 3). These experiments produced mostly $MgSiO_3$ ilmenite or perovskite, with a small amount of carbonate melt in the hot spot. Garnet, if present, was located between the melt and the $MgSiO_3$ phase. The Na content of garnet was the highest at the contact with the melt and lowest at the contact with the $MgSiO_3$ phase. Therefore, two garnet analyses are reported in Table 3 if those two compositions were significantly different. As the limit of the garnet stability was approached, the range of the observed garnet compositions narrowed. The composition of the NaPx–En inclusion was first reproduced by garnet coexisting with $MgSiO_3$ ilmenite and carbonate melt at 21 GPa and 1800°C (run 3352). Since the range of the garnet compositions was still wide, another experiment was carried out at 22 GPa and the same temperature (run 3356). In this case, the range of the garnet compositions was much narrower. Another experiment at 23 GPa and 2000°C produced garnet with the Na content lower than the Na content of the inclusion. The coexisting melt had a much higher silicate component, which diluted its Na content to a level insufficient to impose high enough Na contents on garnet. This suggested that the temperature was too high. In all experiments, the K content of garnet was negligible, indicating that either the pressures were not high enough to produce significant solubility of K in garnet, as observed in [13], or the starting material had the K_2O content too low. Another starting material was prepared with a higher K_2O content and used at 24 GPa and 2000°C (run 3408) and at 23 GPa and 1900°C (run 3412). Garnet was not observed at 24 GPa, perhaps indicating that the pressure was too high for the stability of garnet. However, traces of garnet were found at 23 GPa and 1900°C. The garnet composition closely matched the composition of the NaPx–En inclusion, and had a significant K content only slightly lower than the K content of the inclusion (Table 1). Hence, these experimental conditions are considered to represent the best estimate for the P–T conditions in the source region of the NaPx–En inclusion.

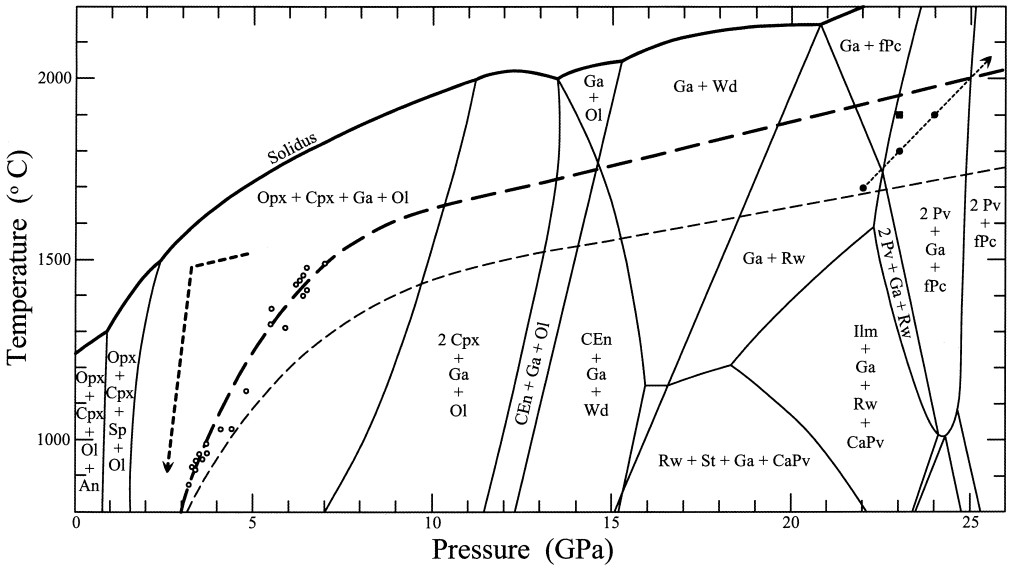

Fig. 3. Temperature–pressure phase diagram for the Earth's mantle (solid lines) based on [39]. The thin dashed line is the previously used geotherm based on [33–35], the heavy dashed line is the geotherm based on the present results. The heavy dotted line shows the *P–T* path recorded by the garnet peridotites of Norway [21]; circles show the *P–T* conditions of equilibration for the garnet lherzolites of northern Lesotho [22]. The square is the best *P–T* estimate for the origin of the NaPx–En inclusion, dots show the experimental *P–T* conditions at which the Ca content of the type III inclusions was matched, and the thin dotted line is the corresponding isopleth. Symbols: An, anorthite; CaPv, $CaSiO_3$ perovskite; CEn, clinoenstatite; Cpx, diopsidic clinopyroxene; fPc, (Mg,Fe)O ferropericlase; Ga, garnet; Ilm, (Mg,Fe)SiO_3 ilmenite; Ol, olivine; Opx, orthopyroxene; Pv, (Mg,Fe)SiO_3 or $CaSiO_3$ perovskite; Rw, $(Mg,Fe)_2SiO_4$ ringwoodite; Sp, $(Mg,Fe)Al_2O_4$ spinel; St, stishovite; Wd, $(Mg,Fe)_2SiO_4$ wadsleyite.

5. Discussion

Fig. 3 shows the *P–T* locations of the experiments in which the Ca content of the type III inclusions was matched. The three experiments mapped out an isopleth of equal Ca contents of garnet coexisting with $CaSiO_3$ perovskite and identical to the Ca content of the inclusions. Since the origin of the type III inclusions should lie on the extrapolation of this isopleth to higher pressures and temperatures, the limit of the garnet stability and, presumably, the stability of TAPP could be reached at a minimum pressure and temperature of 25 GPa and 2000°C. This is consistent with the conditions of origin at 23 GPa and 1900°C for the NaPx–En inclusion. In comparison with the previously used geotherm in Fig. 3, both determinations suggest temperatures in the deep mantle up to 300°C higher. Since the diamonds and inclusions are typically old, it could be argued that these temperatures reflect an Archaean geotherm. However, if the mantle temperatures at the time of the kimberlite eruption were lower, the type III inclusions would exsolve some Ca as $CaSiO_3$ perovskite, and this is not observed. Thus, it is more likely that the present geotherm in the deep mantle is also 300°C higher than the reference geotherm in Fig. 3. The resulting temperatures are higher than predicted by most geotherms for a convecting mantle without a thermal boundary layer at 660 km, but close to the geotherms that include such a thermal boundary layer (e.g. [18,19]). The new geotherm is also close to the geotherm calculated by Ringwood [20] for conduction and radiative heat transfer. Clearly, thermobarometry on inclusions from the transition zone would be most useful in constraining the potential presence of the thermal boundary layer at 660 km. However, the new estimate of the temperatures in the deep mantle is consistent with the high temperatures (1490°C at 3.4 GPa) revealed by the thermobarometry of garnet peri-

dotites from the Western gneiss region of Norway [21], which could be interpreted as a stalled fossil mantle plume. The corresponding adiabat based on these two P–T estimates indicates a potential mantle temperature of 1400°C (Fig. 3). The proposed higher mantle temperatures are also supported by the more recent applications of experimental thermobarometry to garnet lherzolites of northern Lesotho [22], and are in agreement with Kaula [23] and other more recent estimates summarized by Hofmeister [24].

The NaPx–En inclusion appears to have the composition of garnet at the very limit of its stability in depleted (peridotitic) mantle compositions and in equilibrium with percolating carbonate melt. This is shown schematically by the dashed lines in Fig. 1. The coexisting carbonate melt is low in Al, which is thus unavailable to accompany Na into garnet. In contrast, most majoritic garnets observed in high-pressure experiments and those expected to be present in the transition zone would have Al in excess of Na.

Incidentally, the preferred experimental conditions for the origin of the NaPx–En inclusion of 23 GPa and 1900°C are identical to the experimental conditions at which Mg_2SiO_4 ringwoodite breaks down to $MgSiO_3$ perovskite and periclase [14]. This phase transition is considered to be most likely responsible for the 660 km seismic discontinuity. However, in chemically more complex compositions including Fe and Na, and at the higher mantle temperatures indicated by the present study, $(Mg,Fe)_2SiO_4$ ringwoodite breaks down to garnet and ferropericlase at lower pressures [25,26], leaving the transformation from garnet to perovskite as the only other known perovskite-forming reaction capable of producing a discontinuity at 660 km (Fig. 3). Hence, it is possible that the majoritic garnet inclusions with compositions at the limit of their stability, such as the NaPx–En inclusion for peridotite and the type III inclusions for eclogite, represent samples from the boundary between the transition zone and the deep mantle.

Ringwood et al. [27] suggested that kimberlitic melt originated in the transition zone, thus at depths greater than the origin of syngenetic inclusions of majoritic garnet in diamonds. However, since some of the inclusions now appear to come from the deep mantle, it can be expected using the same reasoning that the melt, which brought them to the surface, would also originate in the deep mantle. Ringwood et al. [27] argued that a kimberlite eruption is in some cases a rapid, single-stage process; otherwise the majoritic garnet inclusions would exsolve pyroxene, as is also often observed. The type III and the NaPx–En inclusions both provide evidence in support of this argument. Hutchison [1] described several composite inclusions, including a type III inclusion with TAPP, showing limited or undetectable reaction along the contact between the grains, which could be expected to occur if the inclusions had the opportunity to re-equilibrate within the stability field of majoritic garnet. Similarly, the stability of the NaPx–En inclusion is limited to pressures between 16.5 and 23 GPa, and the inclusion would either transform to an assemblage of two pyroxenes or partially melt, if the ascent and cooling were not rapid and completed while the inclusion still experienced the original confining pressure.

The carbonate melt produced in this study under the deep mantle P–T conditions was extremely ultramafic, highly enriched in K, Na, Fe, Mg, while depleted in Si, Al, and thus very different from the kimberlitic melt. For example, experiments with the same starting composition and at the same temperature of 1600°C (runs 3288 and 3297 in Table 3) produced very different carbonate melt at 22 and 23 GPa. The melt coexisting with $MgSiO_3$ perovskite at 23 GPa had a much higher Na content than the melt coexisting with garnet at 22 GPa. This is the well-known consequence of Na being highly incompatible in perovskite but much more compatible in majoritic garnet [28]. Thus the Na-rich carbonate melt originating in the deep mantle could become kimberlitic while passing through the transition zone by losing Na to majoritic garnet. The resulting metasomatism taking place over a long period of time could have significant cumulative effect on the mineral and chemical composition of the transition zone, presumably exhibiting the strongest effect nearest to the source of the metasomatizing melt.

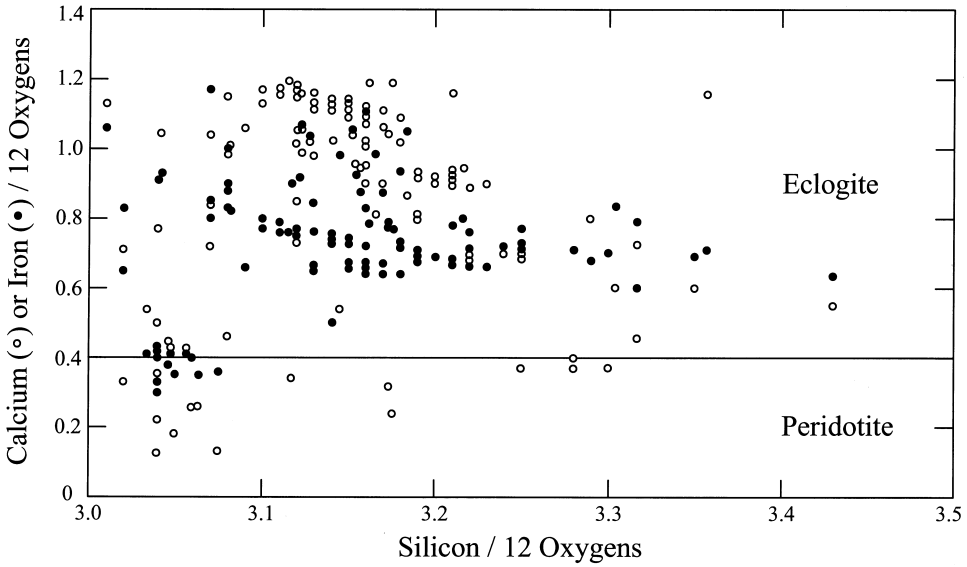

Fig. 4. The plot of Ca (○) or Fe (●) against Si per 12 oxygens of the compositions of majoritic garnet inclusions in diamonds from South Africa [4,36], Brazil [1] and Guinea [1] for the eclogitic Ca- and Fe-rich inclusions, and from China [40] for the peridotitic inclusions low in Ca, Fe and Si.

The process of metasomatism appears to have the potential to produce chemical heterogeneities or hidden reservoirs in the mantle, and could operate continuously in the course of the Earth's history to generate and maintain such heterogeneities even in a highly dynamic Earth. For example, such metasomatism by percolating carbonate melt could produce chemical layering in the upper mantle, with compositional boundaries developing at phase transitions due to the changes in the mineral assemblage and thus in the equilibrium between the melt and the assemblage.

Majoritic garnet inclusions in diamonds provide the best evidence, so far, for the presence of chemical layering. These inclusions were found at several localities worldwide, and most of them have extremely high contents of Ca and Fe (Fig. 4). The Ca content is too high to allow for the presence of enstatite; thus the rock can best be described as eclogite. The high Fe content suggests that this eclogite could have formed by accumulation of the basaltic oceanic crust. The evidence from the majoritic garnet inclusions is consistent with an eclogite-rich layer occurring globally at the depths between 200 and 400 km, thus confirming the predictions by Anderson [29].

The composition of the transition zone between 410 and 660 km is still open to debate. The type III and the NaPx–En inclusions were both considered prime candidates for the transition zone origin. Both turned out to be at best from the very base of the transition zone, and thus not necessarily representative of its mineral and chemical composition. The association of the type III inclusions with other inclusions clearly of the deep mantle origin apparently reflects a common origin due to processes operating in the uppermost region of the deep mantle. Among these, the ferropericlase inclusions are conspicuous by their highly variable Na and Fe contents. Most have negligible Na contents, but a few can have up to 1 wt% of Na_2O [1,30]. These are similar to the experimentally observed Na contents of periclase coexisting with garnet at 20–22 GPa and 2000°C (runs 2627 and 2645 from table 2 in [26]), hence such ferropericlase inclusions could coexist with the type III garnet at the base of the transition zone. In contrast, ferropericlase inclusions with negligible Na contents presumably originated in

the deep mantle in the absence of garnet, and apparently reflect the Na depletion caused by the removal of carbonate melt. The observed high variability in the Fe contents of the ferropericlase inclusions [1,30,31] and the high Al contents revealed by the composite inclusions of the type II perovskite with corundum [1] also suggest that the deep mantle is chemically highly heterogeneous. It is also a region clearly favorable for the formation of diamonds. In contrast, none of the inclusions found so far in diamonds show unambiguous evidence of the origin from within the transition zone. If such inclusions are not found in the future, it would be necessary to explain why the transition zone is not favorable for the formation of diamonds and thus different from the mantle above and below.

6. Conclusions

The *P–T* conditions of origin for the type III inclusions from Brazil and the NaPx–En inclusion from China were experimentally determined and correspond to the base of the transition zone or the uppermost part of the deep mantle. The results provide additional support for the proposals of the deep mantle origin for these and other inclusions reported by Hutchison [1] and others [31,32]. The resulting *P–T* conditions of origin represent the first experimentally determined constraints on the geotherm in the deep mantle and suggest that the temperatures in the deep mantle are about 300°C higher than indicated by a mantle geotherm based on the surface heat flow of 40 mW/m^2 [33] and the 1280°C adiabat [34,35]. The evidence that some of these inclusions required rapid, single-stage transport to the Earth's surface by carbonate melt also points to the deep mantle origin for this melt. Metasomatism of the shallow mantle and the transition zone by Na-rich carbonate melt originating in the deep mantle is recognized as a process that could affect the composition and structure of the mantle and thus potentially play a significant role in its evolution. As a consequence, the two major seismic discontinuities at 400 and 660 km depths could indicate not only phase transitions but also changes in chemical composition.

Acknowledgements

This research was funded by the CSEDI program of the National Science Foundation to T. Gasparik (EAR-9710158) and M.J. Drake (EAR-9706024). The high-pressure experiments reported in this paper were performed in the Stony Brook High Pressure Laboratory, which is jointly supported by the National Science Foundation Science and Technology Center for High Pressure Research (EAR-8920239) and the State University of New York at Stony Brook. Many thanks for the constructive reviews to D.L. Anderson, C. Herzberg and an anonymous reviewer.*[FA]*

References

[1] M.T. Hutchison, The Constitution of the Deep Transition Zone and Lower Mantle Shown by Diamonds and Their Inclusions, Ph.D. Thesis, University of Edinburgh, 1997.
[2] W. Wang, S. Sueno, Discovery of a NaPx–En inclusion in diamond: possible transition zone origin, Miner. J. 18 (1996) 9–16.
[3] K.E. Bullen, An Introduction to the Theory of Seismology, Cambridge University Press, Cambridge, 1947, 276 pp.
[4] R.O. Moore, J.J. Gurney, Pyroxene solid solution in garnets included in diamond, Nature 318 (1985) 553–555.
[5] F.R. Boyd, J.J. Gurney, S.H. Richardson, Evidence for a 150–200 km thick Archaean lithosphere from diamond inclusion thermobarometry, Nature 315 (1985) 387–389.
[6] T. Gasparik, Enstatite–jadeite join and its role in the Earth's mantle, Contrib. Mineral. Petrol. 111 (1992) 283–298.
[7] T. Gasparik, Melting experiments on the enstatite–pyrope join at 80–152 kbar, J. Geophys. Res. 97 (1992) 15181–15188.
[8] T. Gasparik, Melting experiments on the enstatite–diopside join at 70–224 kbar, including the melting of diopside, Contrib. Mineral. Petrol. 124 (1996) 139–153.
[9] J. Harris, M.T. Hutchison, M. Hursthouse, M. Light, B. Harte, A new tetragonal silicate mineral occurring as inclusions in lower-mantle diamonds, Nature 387 (1997) 486–488.
[10] T. Gasparik, Diopside–jadeite join at 16–22 GPa, Phys. Chem. Miner. 23 (1996) 476–486.
[11] T. Gasparik, Transformation of enstatite–diopside–jadeite

pyroxenes to garnet, Contrib. Mineral. Petrol. 102 (1989) 389–405.
[12] T. Gasparik, W. Wang, S. Sueno, Metasomatism of the transition zone revealed by major and trace elements of the NaPx–En garnet inclusion from a diamond, Eos Trans. AGU 80, Spring Meet. Suppl. (1999) S356–357.
[13] W. Wang, E. Takahashi, Subsolidus and melting experiments of a K-rich basaltic composition to 27 GPa: Implication for the behavior of potassium in the mantle, Am. Mineral. 84 (1999) 357–361.
[14] T. Gasparik, Phase relations in the transition zone, J. Geophys. Res. 95 (1990) 15751–15769.
[15] T. Gasparik, The role of volatiles in the transition zone, J. Geophys. Res. 98 (1993) 4287–4299.
[16] T. Gasparik, A temperature-pressure calibration grid for multianvil experiments based on phase relations in the system CaO–MgO–SiO_2, Rev. High Press. Sci. Technol. 7 (1998) 9–11.
[17] T. Gasparik, Evidence for immiscibility in majorite garnet from experiments at 13–15 GPa, Geochim. Cosmochim. Acta 64 (2000) 1641–1650.
[18] R. Jeanloz, F. Richter, Convection, composition and the thermal state of the lower mantle, J. Geophys. Res. 84 (1979) 5497–5504.
[19] S. Spiliopoulos, F. Stacey, The earth's thermal profile: Is there a mid-mantle thermal boundary layer?, J. Geodynamics 1 (1984) 61–77.
[20] A.E. Ringwood, Composition and Petrology of the Earth's Mantle, McGraw-Hill, New York, 1975, 618 pp.
[21] M.P. Terry, P. Robinson, D.A. Carswell, T. Gasparik, Evidence for a proterozoic mantle plume and a thermotectonic model for exhumation of garnet peridotites, Western gneiss region, Norway, EOS Trans. AGU 80, Spring Meet. Suppl. (1999) S359–360.
[22] T. Gasparik, An internally consistent thermodynamic model for the system CaO–MgO–Al_2O_3–SiO_2 derived primarily from phase equilibrium data, J. Geol. 108 (2000) 103–119.
[23] W.M. Kaula, Minimal upper mantle temperature variations consistent with observed heat flow and plate velocities, J. Geophys. Res. 88 (1983) 10323–10332.
[24] A.M. Hofmeister, Mantle values of thermal conductivity and the geotherm from phonon lifetimes, Science 283 (1999) 1699–1706.
[25] J. Zhang, C. Herzberg, Melting experiments on anhydrous peridotite KLB-1 from 5.0 to 22.5 GPa, J. Geophys. Res. 99 (1994) 17729–17742.
[26] T. Gasparik, Y.A. Litvin, Stability of $Na_2Mg_2Si_2O_7$ and melting relations on the forsterite–jadeite join at pressures up to 22 GPa, Eur. J. Mineral. 9 (1996) 311–326.
[27] A.E. Ringwood, S.E. Kesson, W. Hibberson, N. Ware, Origin of kimberlites and related magmas, Earth Planet. Sci. Lett. 113 (1992) 521–538.
[28] C. Herzberg, J. Zhang, Melting experiments on anhydrous peridotite KLB-1: Compositions of magmas in the upper mantle and transition zone, J. Geophys. Res. 101 (1996) 8271–8295.
[29] D.L. Anderson, Chemical stratification of the mantle, J. Geophys. Res. 84 (1979) 6297–6298.
[30] C. McCammon, M. Hutchison, J. Harris, Ferric iron content of mineral inclusions in diamonds from São Luiz: A view into the lower mantle, Science 278 (1997) 434–436.
[31] B. Harte, J.W. Harris, M.T. Hutchison, G.R. Watt, M.C. Wilding, Lower mantle mineral associations in diamonds from São Luiz, Brazil, in: Y. Fei, C. Bertka, B.O. Mysen (Eds.), Mantle Mineralogy: Field Observations and High Pressure Experimentation: A Tribute to Francis R. (Joe) Boyd, The Geochemical Society, Houston, Geochem. Soc. Spec. Publ. No. 6, 1999, pp. 125–153.
[32] B. Scott-Smith, R. Danchin, J. Harris, K. Stracke, Kimberlites near Orrorroo, South Australia, in: J. Kornprobst (Ed.), Kimberlites I: Kimberlites and Related Rocks, Elsevier, Amsterdam, 1984, pp. 121–142.
[33] H.N. Pollack, D.S. Chapman, On the regional variation of heat flow geotherms and lithospheric thickness, Tectonophysics 38 (1977) 279–296.
[34] D. McKenzie, M.J. Bickle, The volume and composition of melt generated by extension of the lithosphere, J. Petrol. 29 (1988) 625–679.
[35] E. Takahashi, Speculations on the Archean mantle: Missing link between komatiite and depleted garnet peridotite, J. Geophys. Res. 95 (1990) 15941–15954.
[36] R.O. Moore, J.J. Gurney, W.L. Griffin, N. Shimizu, Ultra-high pressure garnet inclusions in Monastery diamonds: trace element abundance patterns and conditions of origin, Eur. J. Mineral. 3 (1991) 213–230.
[37] T. Irifune, T. Koizumi, J. Ando, An experimental study of the garnet–perovskite transformation in the system $MgSiO_3$–$Mg_3Al_2Si_3O_{12}$, Phys. Earth Planet. Interact. 96 (1996) 147–157.
[38] T. Kondo, T. Yagi, Phase transition of pyrope garnet under lower mantle conditions, in: M.H. Manghnani, T. Yagi (Eds.), Properties of Earth and Planetary Materials at High Pressure and Temperature, Geophys. Monogr. 101, American Geophysical Union, Washington, DC, 1998, pp. 419–427.
[39] T. Gasparik, A model for the layered upper mantle, Phys. Earth Planet. Interact. 100 (1997) 197–212.
[40] W. Wang, S. Sueno, E. Takahashi, H. Yurimoto, T. Gasparik, Enrichment processes at the base of the Archean lithospheric mantle: observations from trace element characteristics of pyropic garnet inclusions in diamonds, Contrib. Mineral. Petrol. (2000) in press.